Research Article

Impact Force Between Tramcar and Steel Beam Bumper

He Wenhai
Department of Mechanical Engineering, Xi'an University of Science and Technology,
Xi'an, 710054, P.R. China

Abstract: Tramcar will glides fast along inclined railway when it is out of control. Steel beam bumper can prevent its motion. This kind of bumper is widely used in inclined shaft of mine where tramcar is used as auxiliary transport. There exists intense impact between tramcar and steel beam bumper. The impact force is a key parameter for designing bumper. But this force is difficult to predict. Three models are established for obtaining accurately the impact force. In these models, tramcar with its buffer is simplified as a spring-mass system. Steel beam bumper is simplified as Euler-Bernoulli Beam, single-degree-of-freedom spring-mass system and a spring without mass respectively. Simulation shows that impact forces from these models are approximate, so these three models are equivalent. The maximal impact force almost increases linearly with the increasing of mass and impact speed of tramcar. The total impact time increases only with the increasing of mass, but it is not relevant to the impact speed. Single-degree-of-freedom spring-mass model is the simplest one, so it is easy and useful to simulate the impact between tramcar and steel beam bumper for actual engineering design.

Keywords: Bumper, euler-bernoulli beam, impact force, simulation, SIMULINK, tramcar

INTRODUCTION

In mine, Bumper is compelled to install for preventing high speed tramcar from gliding freely along inclined railway (He, 2008). During preventing, there exists intense impact between tramcar and bumper. Actual conditions show that impact force varies with time and its amplitude is very large. Bumper must have enough strength.

There are two kinds of bumper, such as steel beam bumper and flexible bumper. Impact between tramcar and flexible bumper has been simulated (He, 2009). Steel beam bumper shown in Fig. 1 is widely used in China because its structure is simple.

Impact force is a key parameter for designing steel beam bumper, but it is difficult to predict. As a traditional method, amplified gravity of tramcar is used as the impact force. This method is too simple to predict accurately the impact force.

Impact between rigid body and structure has been widely researched (Edwards, 1999; Li *et al*., 2010). Finite Element Method (FEM) and Finite Difference Method (FDM) are used to simulate the impact (Kral, 1993; Yu *et al*., 1996).

The impact between tramcar and steel beam bumper was developed (He and Ren, 2003). And, the deformation of the bumper is neglected. But actual steel beam bumper can deform during impact. The present study develops three models to predict the impact force. In these models, the deformation of steel beam bumper is taken fully into account.
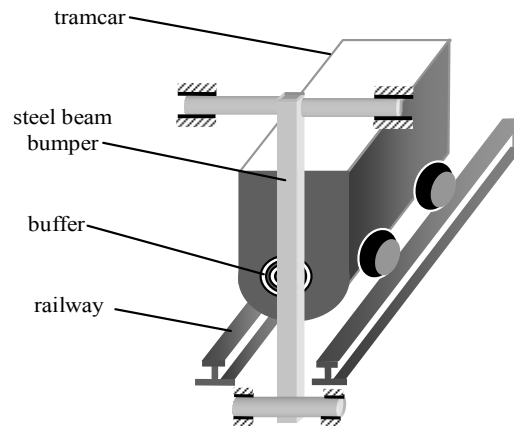

Fig. 1: Tramcar and steel beam bumper

SIMULATION MODEL

Buffer is installed at the front of tramcar and its elastic deformation is very large during impact. Buffer can be equivalent to a spring without mass because its mass is much less than the one of tramcar. The deformation of tramcar can be neglected, so it is reasonable to simplify tramcar as a rigid body whose mass is m_1. Tramcar with buffer can be regarded as spring-mass system.

Steel beam bumper is simplified as three mechanical models in this study, namely Euler-Bernoulli Beam, single-degree-of-freedom spring-mass system and spring without mass.
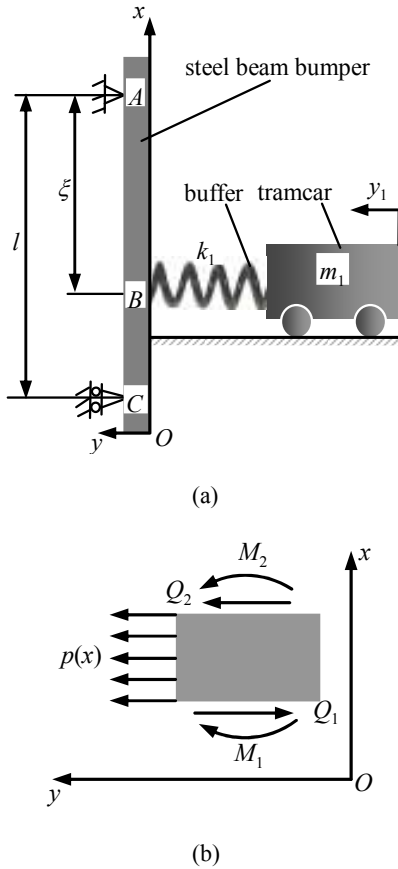
(a)

(b)

Fig. 2: Beam-spring-mass model (a) Impact between tramcar and steel beam bumper, (b) Differential element of steel beam bumper

Three models, such as Beam-spring-mass model, 2-degree-of-freedom spring-mass model and Single-Degree-of-Freedom (SDOF) spring-mass model are used to describe the impact between tramcar and steel beam bumper.

Actual conditions show that tramcar can be rebounded after first impact then impacts the bumper again. The maximal impact force relevant to bumper design exists in the first impact. So, this study simulates the first impact between tramcar and steel beam bumper. Rebound and second impact both are neglected.

Beam-spring-mass model: The main deformation of steel beam bumper is bending when tramcar impacts it. The axis of steel beam bumper and the impact force are in same one plane. The rotation of steel beam bumper is much less and can be neglected. So, steel beam bumper can be regarded as Euler-Bernoulli Beam with equal cross section. Such simplification is reasonable (Thompson and Jones, 2000).

According to above analysis, the corresponding mechanical model is shown in Fig. 2 (a). In this mechanical model, steel beam bumper is supported at points A and C. The touch position between tramcar and steel beam bumper is point B.

The coordinate system is established firstly, x axis coincides with the axis of steel beam bumper. And, its positive direction is upward. Y axis coincides with the motion direction of tramcar.

A differential element of steel beam bumper whose coordinate is $(x, 0)$ is shown in Fig. 2b. And, its displacement is $y (x, t)$ at time t. The dynamics equation satisfies:

$$\rho A dx \frac{\partial^2 y}{\partial t^2} + Q_1 - Q_2 - p(x)dx = 0 \qquad (1)$$

where,

ρ & A : The density and sectional area of steel beam bumper, respectively

$p(x)$: Distribution force acting on steel beam bumper

Q_1 & Q_2 : Shearing force acting on 2 lateral sides of the differential element

Shearing force is continuous, so Q_1 and Q_2 satisfy:

$$Q_2 = Q_1 - \frac{\partial Q_1}{\partial x} dx \qquad (2)$$

Substituting Eq. (2) into (1), yields:

$$\rho A dx \frac{\partial^2 y}{\partial t^2} + \frac{\partial Q_1}{\partial x} - p(x)dx = 0 \qquad (3)$$

Moment acting on the differential element satisfies:

$$M_1 + Q_1 dx - M_2 = 0 \qquad (4)$$

where, M_1 and M_2 are moments acting on 2 lateral sides of differential element.

Moment is continuous, so M_1 and M_2 satisfy:

$$M_2 = M_1 - \frac{\partial M_1}{\partial x} dx \qquad (5)$$

Substituting Eq. (5) into (4) yields:

$$Q_1 = \frac{\partial M_1}{\partial x} \qquad (6)$$

Substituting Eq. (6) into (3) yields:

$$\rho A dx \frac{\partial^2 y}{\partial t^2} + \frac{\partial^2 M_1}{\partial x^2} - p(x)dx = 0 \qquad (7)$$

For beam with equal cross section, the moment satisfies:

$$M_1 = EJ \frac{\partial^2 y}{\partial x^2} \qquad (8)$$

where, E and J are Young's modulus and moment of inertia of steel beam bumper, respectively.

Substituting Eq. (8) into (7) yields:

$$EJ\frac{\partial^4 y(x,t)}{\partial x^4} + \rho A\frac{\partial^2 y(x,t)}{\partial t^2} = p(x,t) \tag{9}$$

It is assumed that the main deformation of bumper satisfies (William and Marie, 2005):

$$y(x,t) = Y(x)\sin(\omega_n t + \varphi_n) \tag{10}$$

where, ω_n and φ_n are the nth natural frequency and phase, respectively. $n = 1, 2, 3\ldots$.

Substituting Eq. (10) into (9) yields:

$$EJY^{(4)} - \omega_n^2 \rho AY = 0 \tag{11}$$

Solution of Eq. (11) satisfies:

$$\begin{aligned}Y(x) &= C_1 \exp(i\alpha x) + C_2 \exp(-i\alpha x)\\ &+ C_3 \exp(\alpha x) + C_4 \exp(-\alpha x)\end{aligned} \tag{12}$$

where, C_1, C_2, C_3, C_4 are parameters, respectively.

$$\alpha_n^4 = \frac{\omega_n^2}{a^2}, \ a^2 = \frac{EJ}{\rho A}$$

Two ends of steel beam bumper are simple supported, so the displacement and moment at their ends are zero. The boundary conditions satisfy:

$$Y(0) = 0, Y(l) = 0, Y''(0) = 0, Y''(l) = 0 \tag{13}$$

where, l is the total length of steel beam bumper.

Substituting Eq. (13) into (12) yields:

$$\left.\begin{aligned} C_1 &= 0\\ C_3 &= 0\\ C_2 \sin\alpha l + C_4 \sinh\alpha l &= 0\\ -C_2 \sin\alpha l + C_4 \sinh\alpha l &= 0 \end{aligned}\right\} \tag{14}$$

It can be obtained from Eq. (14) that:

$$\alpha_n = \frac{n\pi}{l} \tag{15}$$

So, $Y(x)$ satisfies:

$$Y_n(x) = C_n \sin\frac{n\pi x}{l} \tag{16}$$

Normalization is used to obtain parameter C_n:

$$\int_0^l C_n \sin\frac{n\pi x}{l} = 1 \tag{17}$$

The nth modal of simple supported steel beam bumper satisfies:

$$Y_n = \sqrt{\frac{2}{\rho A l}} \sin\frac{n\pi x}{l} \tag{18}$$

The displacements of every point on the steel beam bumper satisfy:

$$y(x,t) = \sum_{n=1}^{\infty} Y_n(x) q_n(t) \tag{19}$$

where, $q_n(t)$ is the nth normal coordinate corresponding to $Y_n(x)$.

Substituting Eq. (19) into (9), yield:

$$\sum_{n=1}^{\infty} \rho A Y_n \ddot{q}_n + \sum_{n=1}^{\infty} EJ\frac{d^4 Y_n}{dx^4} q_n = p(x,t) \tag{20}$$

It is known from the actual conditions that the impact force applied to steel beam bumper is concentrated force. But the right hand of Eq. (9) is distributed force, so it is necessary to transform the concentrated force to the distributed one, namely:

$$p(x,t) = P(t)\delta(x-\xi) \tag{21}$$

where ξ is the distance between the upward supported end and the impact point on steel beam bumper.

Substituting Eq. (21) into (20), yields:

$$\sum_{n=1}^{\infty} \rho A Y_n \ddot{q}_n + \sum_{n=1}^{\infty} EJ\frac{d^4 Y_n}{dx^4} q_n = P(t)\delta(x-\xi) \tag{22}$$

Two sides of Eq. (22) are multiplied by $Y_m(x)$, then integrated with respect x along the length of steel beam bumper, yields:

$$\begin{aligned}&\int_0^l \sum_{n=1}^{\infty} \rho A Y_m Y_n \ddot{q}_n dx + \int_0^l \sum_{n=1}^{\infty} EJ Y_m \frac{d^4 Y_n}{dx^4} q_n dx\\ &= \int_0^l P(t)\delta(x-\xi)dx\end{aligned} \tag{23}$$

For Bernoulli-Euler beam, its modal satisfies (William and Marie, 2005):

$$\int_0^l \rho A Y_i Y_j dx = \delta_{ij} \tag{24}$$

$$\int_0^l Y_i \left(EJ Y_j''\right)'' = -\omega_n^2 \delta_{ij} \tag{25}$$

where, δ_{ij} is equal to 1 if $i = j$, otherwise δ_{ij} is equal to 0. According to Eq. (24) and (25), Eq. (23) can be rewrite as:

$$\ddot{q}_n(t) + \frac{EJ}{\rho A}\left[\frac{n\pi}{l}\right]^4 q_n(t) = P(t)Y_n(\xi) \tag{26}$$

For obtaining $q_n(t)$, 2 inertial conditions are necessary. It is assumed that these conditions satisfy:

$$y(x,0) = f_1(x) \tag{27}$$

$$\left.\frac{\partial y}{\partial t}\right|_{t=0} = f_2(x) \tag{28}$$

Equation (27) and (28) are multiplied by $\rho A Y_n(x)$ and integrated with respected x along the length of steel beam bumper, yields:

$$q(t) = \int_0^l \rho A f_1(x) Y_n(x) dx \tag{29}$$

$$\dot{q}(t) = \int_0^l \rho A f_2(x) Y_n(x) dx \tag{30}$$

So, normal coordinate satisfies:

$$q_n(t) = q_n(0)\cos\omega_n t + \frac{\dot{q}(t)}{\omega_n}\sin\omega_n t$$
$$+ \frac{1}{\omega_n}\int_0^t\int_0^l p(x,t)Y_m(x)\sin\omega_n(t-\tau)dxd\tau \tag{31}$$

The displacement of the impact point on steel beam bumper satisfies:

$$y(\xi,t) = \sum_{n=1}^{10} Y_n(\xi)q_n(t) \tag{32}$$

Because tramcar with buffer is simplified as a spring-mass system, so its dynamics equation of satisfies:

$$m_1\ddot{y}_1(t) + k_1[y_1(t) - y(\xi,t)] = 0 \tag{33}$$

where,
m_1 & y_1: Mass and the displacement of tramcar, respectively
k_1 : The stiffness coefficient of buffer

The impact force between tramcar and steel beam bumper satisfies:

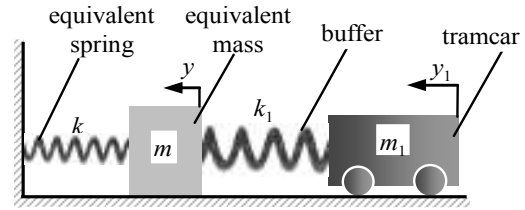$$F(t) = k_1[y_1(t) - y(\xi,t)] \tag{34}$$

Fig. 3: Two-degree-of-freedom spring-mass model

Two-degree-of-freedom spring-mass model: Mass and stiffness of steel beam bumper are continuous. According to the principles of equivalent mass and equivalent stiffness, steel beam bumper can be simplified as signal-degree-of-freedom spring-mass system. And, it is composed of a spring without mass and a rigid body whose mass is m. So, tramcar with its buffer and steel beam bumper can consist of 2-degree-of-freedom spring-mass system. The corresponding mechanical model is shown in Fig. 3.

According to above mechanical model, the corresponding dynamics equation satisfies:

$$\begin{bmatrix} m_1 & 0 \\ 0 & m \end{bmatrix}\begin{Bmatrix} \ddot{y}_1 \\ \ddot{y} \end{Bmatrix} + \begin{bmatrix} k_1 & -k_1 \\ -k_1 & k+k_1 \end{bmatrix}\begin{Bmatrix} y_1 \\ y \end{Bmatrix} = \begin{Bmatrix} 0 \\ 0 \end{Bmatrix} \tag{35}$$

where,
m & k : The equivalent mass and stiffness of steel beam bumper, respectively
y : The displacement of the impact point on steel beam bumper

It is assumed that the displacement of point B under impact force is similar to the one under static loading P. So, the deflection between point A and point B satisfies (Mott, 2002):

$$y_{AB}(x) = \frac{P\xi^2(l-\xi)^2}{3EJl}\frac{l^3}{2\xi^2(l-\xi)}\left[\frac{\beta x}{l} - \frac{(l-\xi)^2 x}{l^3}\right] \tag{36}$$

where, β is coefficient relevant to ξ.
And, the deflection between point B and point C satisfies:

$$y_{BC}(x) = \frac{P\xi^2(l-\xi)^2}{3EJl}\frac{l^3}{2\xi(l-\xi)^2}\left[\frac{\beta x}{l} - \frac{\xi^2 x}{l^3}\right] \tag{37}$$

The equivalent mass of steel beam bumper satisfies:

$$m = \rho\int_0^\xi [f_1(x)]^2 dx + \rho\int_\xi^{l-\xi} [f_2(x)]^2 dx \tag{38}$$

where,

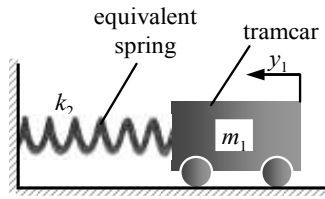$$f_1(x) = \frac{l^3}{2\xi^2(l-\xi)}\left[\frac{\beta x}{l} - \frac{(l-\xi)^2 x}{l^3}\right]$$

Fig. 4: Single-degree-of-freedom spring-mass model

$$f_2(x) = \frac{l^3}{2\xi(l-\xi)^2}\left[\frac{\beta x}{l} - \frac{\xi^2 x}{l^3}\right]$$

The equivalent stiffness of steel beam bumper satisfies:

$$k = \frac{EJl}{\xi^2(l-\xi)^2} \tag{39}$$

The force between the equivalent mass and the tramcar satisfies:

$$F(t) = k_1[y_1(t) - y(t)] \tag{40}$$

Single-degree-of-freedom spring-mass model: Mass of steel beam bumper is much less than the one of tramcar, so it is reasonable to neglect the equivalent mass of steel beam bumper in the 2-degree-of-freedom model. The equivalent spring of steel beam bumper and buffer can connect in series. A new Single-Degree-of-Freedom (SDOF) spring-mass mechanical model is shown in Fig. 4.

According to Newton's second law, the corresponding dynamics equation satisfies:

$$m_1\ddot{y}_1 + k_2 y_1 = 0 \tag{41}$$

The stiffness of spring k_2 satisfies:

$$k_2 = \frac{kk_1}{k + k_1} \tag{42}$$
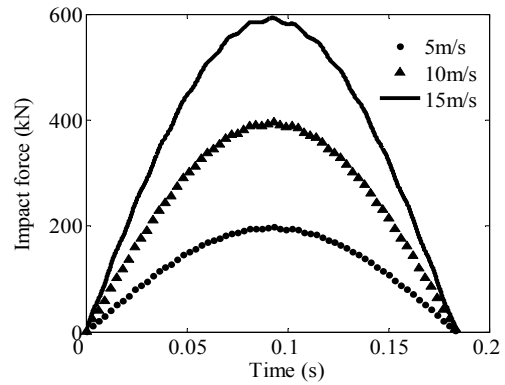
Substituting Eq. (39) into (42), yields:

$$k_2 = \frac{3EJkl}{3EJl + k\xi^2(l-\xi)^2} \tag{43}$$
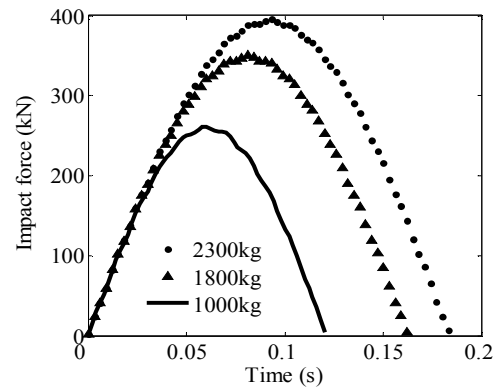
According to this model, the impact force satisfies:

$$F(t) = k_2 y_1(t) \tag{44}$$

SIMULATION AND ANALYSIS

SIMULINK/MATLAB is used in the present study for simulation. The modules which are connected by

(a)

(b)

Fig. 5: Impact force from beam-spring-mass model (a) impact force when impact speed of tramcar is different, (b) impact force when mass of tramcar is different

lines represent program codes in SIMULINK. And, data can flow between the modules through lines (Wan *et al.*, 2009).

According to actual conditions, Young's modulus of steel beam bumper is 209 Gpa and its moment of inertia is 2.51×10^{-6} kg/m^2, sectional area is 1.5×10^{-3} m^2, mass density is 7.8×10^3 kg/m^3, total length is 2 m, the distance between impact point and upward end is 1.65 m, the stiffness coefficient of buffer is 7.90×10^5 N/m.

Impact force from beam-spring-mass model: It is assumed that tramcar whose mass is 2300 kg impacts steel beam bumper with different impact speed, such as 5, 10 and 15 m/s, respectively. For their first impact, it is known from Fig. 5a that impact force increases from zero and reaches peak at about 0.09s, then it decreases to zero. The peak of impact force increases with the increasing of impact speed. But the total impact time does not vary with impact speed.

It is assumed that three different tramcars whose mass are 1000, 1800 and 2300 kg impact steel beam bumper with same impact speed 10 m/s. For their first impact, it is known from Fig. 5b that the impact force increases from zero and reaches peak at different time.
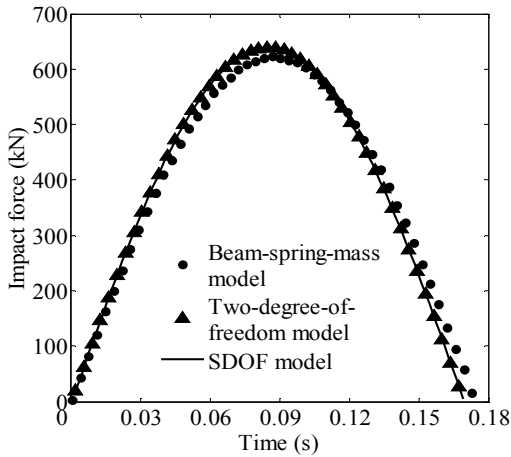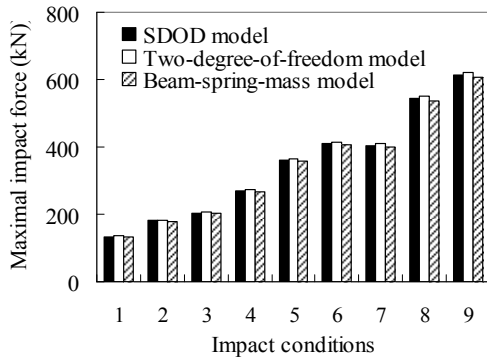
Fig. 6: Impact force from three models

Fig. 7: Maximal impact force from three models corresponding to nine impact conditons

Table 1: Impaction conditions

Impaction condition	Mass of tramcar (kg)	Impact speed (m/s)
1	1000	5
2	1800	5
3	2500	5
4	1000	10
5	1800	10
6	2500	10
7	1000	15
8	1800	15
9	2500	15

And, the peak of impact force and total impact time increase with the increasing of mass of tramcar.

Impact force from three models: It is assumed that tramcar whose mass and impact speed are 2500 kg and 15 m/s, respectively. The impact forces from above three models are shown in Fig. 6. All these impact forces are approximate. So, these 3 models are equivalent. The SDOF spring-mass model is the simplest one, so it is easy to use this model to simulate the impact between tramcar and steel beam bumper.

The maximal impact force that exists in the first impact is an important parameter for designing bumper.
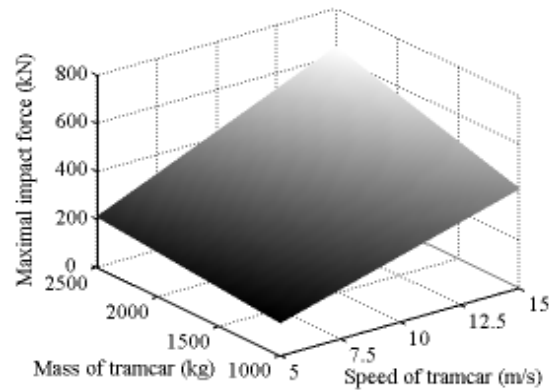

Fig. 8: Maximal impact force depends on mass and impact speed of tramcar

For obtaining the characteristic of maximal impact force, it is assumed that there are three tramcars whose mass are 1000, 1800 and 2500 kg, respectively. All these tramcars impact steel beam bumper with three impact speeds, namely 5, 10 and 15 m/s. These masses and impact speeds comprise nine impact conditions shown in Table 1.

It is known from Fig. 7 that the maximal impact force depends on mass and impact speed of tramcar. And, these forces from three models corresponding to nine impact conditions are approximate. So, these three models are equivalent. In Fig. 8, the maximal impact force almost increases linearly with the increasing of the mass and impact speed of tramcar.

CONCLUSION

According to actual conditions, three models are used to simulate the impact between tramcar and steel beam bumper. Simulation shows that these models are equivalent and the impact forces from these models are approximate. In these three models, the SDOF spring-mass model is the simplest one. It is easy and helpful for actual engineering design.

The maximal impact force is a key parameter for steel beam bumper design. And, it almost increases linearly with the increasing of mass and impact speed of tramcar.

ACKNOWLEDGMENT

REFERENCES

Edwards, J.R., 1999. Finite element analysis of the shock response and head slap behavior of a hard disk drive. IEEE Trans. Magn. , 35(2): 863-86.

He, W.H. and Z.Q. Ren, 2003. Dynamics of tramcar-runaway prevention device based on MATLAB. Mine Machine No., 7: 53-55.

He, W.H., 2008. Modeling and simulative analysis of dynamics characteristic of tramcar conveying system. J. Syst. Simul., 20(4): 871-873.

He, W.H., 2009. Simulation research on impaction between tramcar and flexible bumper. International Conference on Electronic Computer Technology, pp: 569-573.

Kral, F.R., 1993. Elastic-plastic finite element analysis of re-peated indentation of a half-space by a rigid sphere. J. Appl. Mech., 60(4): 829-841.

Li, Y.W., F.F. Xi and K. Behdinan, 2010. Dynamic modeling and simulation of percussive impact riveting for robotic automation. J. Comput. Nonlinear Dyn., 5(2):1-10.

Mott, R.L., 2002. Applied Strength of Materials. 4th Edn., Prentice Hall, New Jersey.

Thompson, D.J. and C.J.C. Jones, 2000. A review of the modeling of wheel/rail noise generation. J. Sound Vib., 231(3): 519-536.

Wan, C.X., J.X. Dong, Liu Y.F., Hu H., 2009. Optimized controller for electrostatic force feedback micro accelerometers. J. Tsinghua Univ., 49(11): 1779-1782.

William, T.T. and D.D. Marie, 2005. Theory of vibration with applications. Prentice Hall, New Jersey.

Yu, T.X., J.L. Yang and S.R. Reid, 1996. Dynamic behaviour of elastic-plastic free-free beams subjected to impulsive loading. Int. J. Solids Struct., 33(18): 2659-2680.